The Pharma Innovation Journal 2023; SP-12(12): 1922-1928

www.ThePharmaJournal.com

The Pharma Innovation

ISSN (E): 2277-7695
ISSN (P): 2349-8242
NAAS Rating: 5.23
TPI 2023; SP-12(12): 1922-1928

www.thepharmajournal.com
Received: 07-09-2023
Accepted: 11-10-2023

Salam Jayachitra Devi
ICAR-National Research Centre on Pig, Guwahati, Assam, India

Jaya Bharati
ICAR-National Research Centre on Pig, Guwahati, Assam, India

NH Mohan
ICAR-National Research Centre on Pig, Guwahati, Assam, India

Corresponding Author:
Salam Jayachitra Devi
ICAR-National Research Centre on Pig, Guwahati, Assam, India

Multiclass cell segmentation using a pixel classification algorithm

Salam Jayachitra Devi, Jaya Bharati and NH Mohan

Abstract
Image segmentation is a critical task in biological image analysis, providing essential information for various biomedical applications. Manual segmentation, though accurate, is time-consuming and impractical for big image data. In this study, we analyze an automated approach to enhance live and apoptotic cell segmentation using FIJI, a popular open-source image processing platform. This method leverages supervised learning algorithm based on pixel classification with different filters to achieve precise and efficient segmentation of cells in complex biological images. Experiments were conducted on different image data such as pig luteal cell microscopy image with trypan blue stain and without stain. Comparative analysis of the results obtained from different filters with manual segmentation is performed. From the analysis, the pixel-based classification algorithm performs better in case of image with trypan blue stain that achieved sensitivity of 0.93% for apoptotic cell and 0.86% for live cell. Average IoU score of pixels based segmented cells to manual segmented cells is above 0.91 for apoptotic cell and 0.80 for live cell. This paper contributes to the field by providing a comprehensive framework for automated cell segmentation in FIJI, paving the way for improved efficiency in biological image analysis. The method not only enhances segmentation accuracy but also showcases the potential for wider applicability in diverse biological imaging contexts.

Keywords: Segmentation, FIJI, pixel classification, machine learning, random forest

Introduction
The accurate segmentation of cells from complex biological images is a fundamental requirement for various applications in the realm of biomedical research, including cellular biology, pathology, and drug discovery. The meticulous delineation of individual cell provides crucial insights into cellular processes, aiding in the understanding of disease mechanisms and facilitating the development of targeted therapies. However, the traditional approach of manual cell segmentation is not only time-consuming but also prone to subjectivity and variability, especially when dealing with image data with multiple objects [1-4]. The need for efficient and reproducible segmentation methods has led to a growing interest in automated techniques. Among the diverse array of image processing platforms, FIJI (Fiji Is Just ImageJ) has emerged as a powerful and widely adopted tool in the biological imaging community. Developed as an open-source platform, FIJI offers a comprehensive set of features and plugins, making it suitable for a broad range of image analysis tasks [6-7]. As the demand for automated segmentation methods intensifies, the integration of sophisticated algorithms within platforms like FIJI becomes pivotal for advancing the field of biological image analysis.

FIJI provides a range of traditional image segmentation techniques that have been the foundation in various scientific investigations. Thresholding is a fundamental technique in image segmentation, involving the classification of pixels based on intensity values [8]. FIJI offers a variety of thresholding algorithms, such as Otsu's method [9] and the Triangle method [10]. These methods are widely employed for their simplicity and effectiveness in scenarios with distinct intensity differences. Region growing algorithms [11], available in FIJI, start with seed points and expand regions based on pixel similarity. This method is valuable for segmenting structures with locally homogeneous characteristics. The watershed transformation [12] is employed for segmenting images with complex structures or overlapping objects. FIJI's watershed segmentation allows researchers to identify markers and delineate regions based on intensity gradients, contributing to the precise segmentation of distinct objects. FIJI incorporates edge detection algorithms, including the Canny edge detector [13]. Edge detection is beneficial for identifying boundaries within an image. FIJI has been extensively utilized in cellular biology for segmenting cell structures in microscopy images.

A study by Schindelin *et al*. showcases the application of FIJI in the segmentation of cells, emphasizing its user-friendly interface and adaptability to diverse experimental setups [6]. In neuroscience, FIJI has been employed for segmenting and analyzing neuronal structures in brain imaging. FIJI finds applications in medical imaging and pathology [14]. Image segmentation is crucial for identifying regions of interest in diagnostic images. Studies by Preibisch *et al*., showcase the use of FIJI for segmenting large 3D image datasets, emphasizing its role in volumetric image analysis [7]. Saalfeld *et al*. demonstrated the integration of machine learning techniques within FIJI for neuron segmentation, highlighting the platform's adaptability to cutting-edge methodologies [15]. FIJI allows the incorporation of custom machine learning models and offers plugins, such as Trainable Weka Segmentation, enabling researchers to train classifiers for specific segmentation tasks [16]. This integration enhances FIJI's capabilities by allowing adaptive learning from image datasets. A study by Arganda-Carreras *et al*. [16] demonstrated the application of machine learning-based algorithms, including TWS, for the segmentation of biological structures in microscopy images. The use of machine learning allows these algorithms to adapt to variations in image characteristics and achieve high segmentation accuracy. Research by Ronneberger *et al*. introduced the U-Net architecture, a convolutional neural network (CNN) specifically designed for biomedical image segmentation. The U-Net architecture incorporates a contracting path for capturing context and a symmetric expanding path for precise localization, making it well-suited for tasks such as cell segmentation [5]. While CNNs, including U-Net, have shown remarkable success in various segmentation tasks, their complexity and computational requirements can limit their applicability, especially for real-time or resource-constrained scenarios. In a study a pixel classification algorithm based on random forests was employed for the segmentation of cervical cell images. The algorithm demonstrated robust performance in dealing with variations in cell appearance, contributing to the efficiency of high-throughput analysis in cytological screening [17]. This enhanced the potential of pixel classification algorithms in addressing challenges related to cell heterogeneity and diverse imaging conditions. Despite the progress in automated segmentation methods, challenges persist. Variations in image size, cell size, shape, and staining intensity, as well as the presence of artifacts, necessitate continuous advancements in segmentation algorithms. Furthermore, the lack of a universal solution highlights the need for analysis of context-specific approaches that can adapt to different biological imaging tasks. In this context, pixel classification algorithms have garnered attention for their ability to assign pixels to predefined classes based on learned features by improving the precision of cell segmentation. This supervised machine learning-based algorithms allows to adapt to diverse biological images and imaging conditions pose significant challenges for accurate segmentation. This study seeks to address the challenges by analyzing an enhanced cell segmentation approach using FIJI and leveraging a pixel classification algorithm. These algorithms typically involve training a classifier with different filters on labeled data, allowing it to learn the characteristics of different cell types and structures. The primary objectives of this research are two-fold: firstly, to analyze a pixel classification algorithm within the FIJI framework considering different filters for automated cell segmentation, and secondly, to rigorously evaluate the performance of the approach against manual segmentation.

Methodology

Design of multiclass image segmentation

The general process for multiclass image segmentation using the open-source software Fiji [18] is illustrated in Figure 1. Fiji offers various tools for segmenting molecular images, and in this context, it provides a machine learning-based interface for segmenting image volumes of any size and dimension. The image processing encompasses both trypan blue stain and unstain images.

In this segmentation approach, a manual annotation of a subset of objects from each class is carried out using Fiji's drawing tools. It is noteworthy that the annotation doesn't need to cover the entire image, deviating from traditional methods that require annotation for the entire image, a time-consuming task especially unsuitable for large datasets with numerous objects. The Fiji Pixel classification algorithm proves to be well-suited for efficiently segmenting extensive image data containing multiple objects. Following the annotation of selected objects, users choose pixel classification settings and select filters provided in the settings. The analysis incorporates diverse filters, including a basic filter comprising Gaussian blur, Gaussian gradient magnitude, Laplacian of Gaussian, and Hessian eigenvalues. Additionally, Sobel filter, Gabor filter, and Structure Tensor eigenvalues are employed, all executed with sigma values of 1, 2, 4, and 8. Upon selecting the filters, training is executed using a random forest classifier. The outcome is a segmented image representing different classes. Further enhancement involves applying color contrast techniques to distinguish live and apoptotic cells distinctly within the segmented image. To evaluate the classifier's performance with different filters, the segmented images undergo the mask instant comparator method. This comprehensive procedure ensures a robust and efficient segmentation process, particularly applicable to large image datasets with diverse objects. The worflow of the study is illustrated in fig.1.

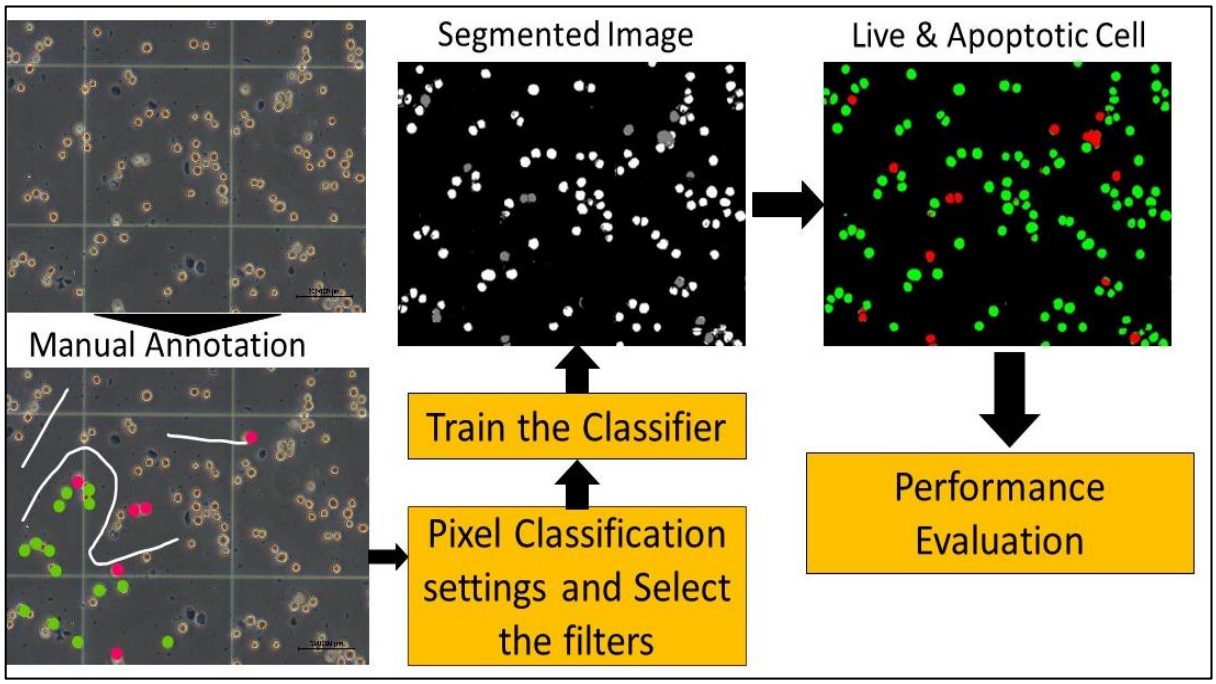

Fig 1: Multiclass cells segmentation using pixel classification

Pixel based classification algorithm

The automatic cell image segmentation using pixel classification algorithm uses random forest classifier to classify each pixel independently. Random forest classifier [19] is a commonly used supervised learning method that can be trained on pre labeled pixels i.e., Live Cell, Apoptotic Cell and Background. In the pixel classification algorithm, the random forest is trained on few manually labeled multiclass pixels. This approach can handle big image data. The first step computes a feature vector for each labeled pixel in the image. The feature vectors are generated by applying a set of filters to the given input images. Some of the filters used in the image analysis are basic filters that include gaussian blur, gaussian gradient magnitude, Laplacian of gaussian, and hessian eigen values, Sobel filter, Gabor filter and Structure tensor eigenvalues with sigma values 1, 2, 4 and 8. A stack of feature is built by adding each pixel to their feature vector. The feature vectors generated are paired with their respective ground truth classes that constitute the training feature set. Later each pixel's feature vector is fed into the random forest for training, which then predicts the probability of the pixel belonging to a particular class. The random forest classifier used in this training procedure consists of 100 decision trees [18]. This segmentation process utilizes the learned relationships from the training phase to categorize pixels throughout the entire image. The result is a segmented image where each pixel is assigned a probability of belonging to either Live Cell, Apoptotic Cell and Background.

Feature extraction

The pixel classification algorithm relies on selection of filters to compute pixel features with a designated list of sigma values. These sigma values play a crucial role in shaping the behavior of the filters. The input to the algorithm consists of an image I and list of sigma values (such as $\sigma_1, \sigma_2 \ldots \sigma_N$) and a directive indicating the input image processing for 2D. For 2D, the size of the pixels x and y be denoted by w_x and w_y where $w_x = w_y = 1$. The purpose of sigma value in the list is to blur the input images according to gaussian filter resulting to N differently blurred images of the given input images denoted by G_i [18, 20].

$$G_i = gaussian_i I, \text{ for } i = 1, \ldots, N$$

Where, $G_0 = I$ denotes the original image. The first order partial derivatives of the given image with x and y pixel is denoted by $\delta_x G_i$ and $\delta_y G_i$. They are computed by using the following mathematical expression.

$$\delta_x G_i = \frac{1}{w_x}[-0.5\ 0\ 0.5] * G_i$$

Likewise, the second order derivative of the given input image is denoted as $\delta_x^2 G_i$ and they are computed as

$$\delta_x^2 G_i = \frac{1}{w_x^2}[1\ -2\ 1] *\ G_i$$

Mixed second order derivative of the given input image is denoted as $\delta_x \delta_y G_i$ and computed as

$$\delta_x \delta_y G_i = \frac{1}{w_y} - [-0.5\ 0\ 0.5]_y * (\frac{1}{w_x}[-0.5\ 0\ 0.5]_x * G_i)$$

Gaussian Blur [16]: The mathematical expression of gaussian blur resulting to N images of gaussian blurred of the given input images is as follows

$$f_i^{guas} = G_i \text{ for } i = 1, \ldots . N$$

Gaussian Gradient Magnitude [16]: It produces $N + 1$ output images for each G_i where $i = 0, \ldots . N$. The magnitude of the gradient vector for each pixel is used to generate the output image and the mathematical expression is as follows

$$f_i^{ggm} = \sqrt{(\delta_x G_i)^2 + (\delta_y G_i)^2}\ (= |grad\ G_i|)$$

Laplacian of Gaussian [16]: It also produces $N + 1$ output images for each G_i where $i = 0, \ldots . N$. The resulting output is

the total of second order partial derivatives and represented as

$$f_i^{lg} = \delta_x^2 G_i + \delta_y^2 G_i$$

Hessian Eigenvalues [16]: It produces $2(N+1)$ output images i.e. two images for each G_i where $i = 0, \ldots . N$. Initially, second order partial derivatives are calculated as

$$h^{xx} = \delta_x^2 G_i \; h^{yy} = \delta_y^2 G_i \; h^{xy} = h^{yx} = \delta_x \delta_y G_i$$

These partial derivatives for each pixel u can be represented in matrix form as

$$h_u = \begin{bmatrix} h^{xx}(u) & h^{xy}(u) \\ h^{yy}(u) & h^{yx}(u) \end{bmatrix}$$

and the filter computes two eigenvalues for this matrix and written pixel by pixel into two output images as
$f_1^h(u) = \lambda_{1,u}$ and $f_2^h(u) = \lambda_{2,u}$

Structure Tensor Eigenvalues [16]: In this filter four images $4(N+1)$ for each G_i where $i = 0, \ldots . N$ is generated. The four output images are calculated on different integration scale as two images are calculated with parameter $\gamma = 1$ and another two are calculated with $\gamma = 3$. To compute pixel wise product for first order derivatives is as follows

$p^{xx} = \delta_x G_i . \delta_x G_i$, $p^{xy} = \delta_x G_i . \delta_y G_i$, $p^{yx} = \delta_y G_i . \delta_x G_i$, and $p^{yy} = \delta_y G_i . \delta_y G_i$

Then gaussian blur $\sigma = \gamma$ are used to blue these images as $q_\gamma^{xx} = gaussian_i p^{xx}$, $q_\gamma^{yy} = gaussian_i p^{yy}$, $q_\gamma^{yx} = gaussian_i p^{yx}$ and $q_\gamma^{xy} = gaussian_i p^{xy}$
Further, the four-blur image for each pixel u in the given image are sampled into matrix as

$$q^u = \begin{bmatrix} q_\gamma^{xx}(u) & q_\gamma^{xy}(u) \\ q_\gamma^{yy}(u) & q_\gamma^{yx}(u) \end{bmatrix}$$

The filter computes two eigenvalues for this matrix and written pixel by pixel into two output images as $f_1^{ste}(u) = \lambda_{1,u}$ and $f_2^{ste}(u) = \lambda_{2,u}$

Gabor [22]: The 2-D Gabor filter is characterized by the convolution of a Gaussian function and a complex sinusoidal waveform that varies in frequency and orientation. It is computed as

$$G(x,y) = e^{-\frac{(x-x_0)^2}{2\sigma_x^2} - \frac{(y-y)^2}{2\sigma_y^2}} \; e^{j(w_{xo}x + w_{yo}y)}$$

where w_{xo} and w_{yo}denotes centre frequency in which the filter produces the greatest response of x and y. σ_x and σ_y denotes the standard deviation of the Gaussian function and x, y represent the pixel position of the image.

Sobel [21]: In Sobel the gradient of a 2D function $f(x,y)$ is denoted by the vector $\nabla f = [Gx, Gy]$, where Gx and Gy represents first derivative and its magnitude is represented as $\| \nabla f \| = [Gx^2 + Gy^2]^{1/2}$. The key characteristic of the gradient vector is that it points toward the direction of the greatest rate of change of the function f at the coordinates (x,y). The angle at which the maximum rate of change occurs is given by $\alpha(x,y) = \arctan(\frac{Gy}{Gx})$.

Metrics
Recall, Intersection over Union (IoU), and F-measure are commonly used metrics in the evaluation of classification and object detection tasks.
Recall [23]: It is also known as sensitivity or true positive rate that measures the ability of a model to correctly identify all relevant instances within a dataset. It is calculated as the ratio of true positives to the sum of true positives and false negatives:

$$Recall = \frac{True\ Positives}{True\ Positives + False\ Negatives}$$

High recall indicates that the model is effective in capturing a large proportion of the positive instances.
Intersection over Union (IoU) [24]: IoU is commonly used in the context of object detection and segmentation tasks. It measures the overlap between the predicted segmentation and the ground truth segmentation. The IoU is calculated as the ratio of the intersection area to the union area of the two segmented images: $IoU = \frac{Intersection\ Area}{Union\ Area}$ values range from 0 to 1, where a higher IoU indicates better spatial overlap between the predicted and true segmented area.
F-measure [25]: The F-measure combines precision and recall into a single metric. It is particularly useful when there is an uneven class distribution. The F1 score is the harmonic mean of precision and recall, and it provides a balance between the two: $F\ Measure = \frac{2 * Precision * Recall}{Precision + Recall}$. It ranges from 0 to 1, with higher values indicating a better trade-off between precision and recall.

Results and Discussion
In this work, we demonstrated an automatic process for luteal cell image segmentation using open-source scientific image analysis platform, FIJI. In this analysis, microscopic cell images of trypan blue stain and unstain image data were used and it is shown in figure 2.

The Pixel classification algorithm is utilized for the automated segmentation and classification of live and apoptotic cells. The process involves annotating a few objects and executing the random forest classification algorithm. The algorithm operates on various filters, including Gaussian blur, Gaussian gradient magnitude, Laplacian of Gaussian, Hessian eigenvalues, Sobel filter, Gabor filter, and Structure tensor eigenvalues with sigma values of 1, 2, 4, and 8. To assess its performance, we conducted experiments on ten stained and unstained images, respectively. The evaluation was based on recall, Intersection over Union (IoU), and F-measure metrics. The average performance metric values for each filter were calculated from the results obtained in the experiments on the ten images. The final outcomes were summarized in Tables 1 and 2.

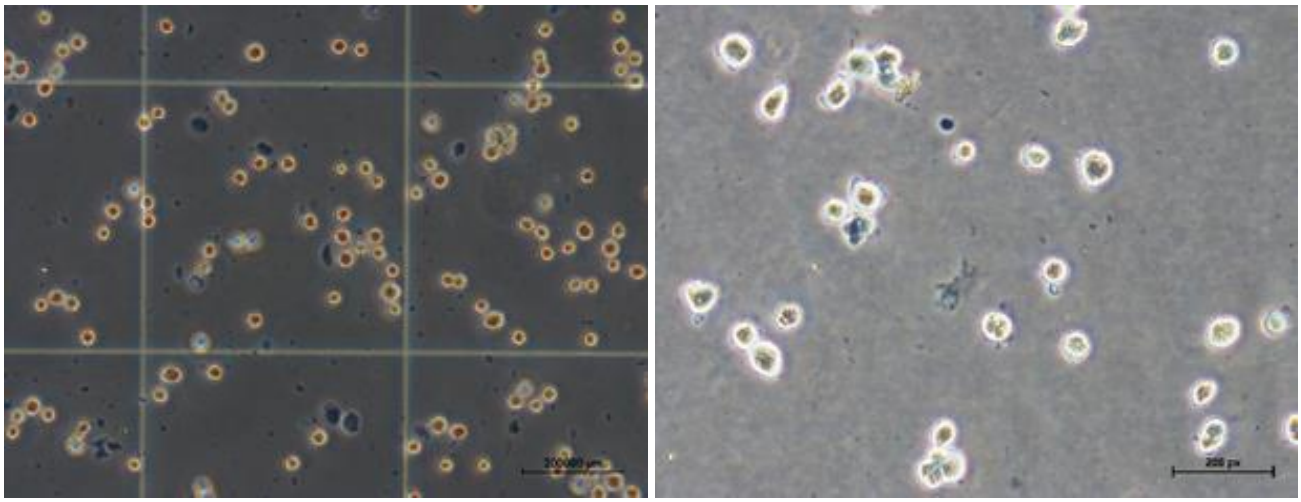

(a) (b)

Fig 2: (a) Trypan blue stain luteal cell image (b) Unstain luteal cell image

In Table 1, the results obtained from trypan blue stain images were depicted, whereas Table 2 presented the results for unstain images. The performance metrics for live and apoptotic cells were computed separately and displayed accordingly. Notably, Table 1 indicated that the basic filter outperformed other filters, achieving performance consistently above 0.80 in recall and IoU metrics. However, it exhibited lower performance in the case of apoptotic cells, particularly with the F-measure metric.

Similarly, in Table 2, the algorithm's performance was assessed for unstain images based on recall, IoU, and F-measure. Interestingly, the algorithm exhibited superior performance in the segmentation of live and apoptotic cells of trypan blue stained images compared to unstained images. Consequently, the segmented images from trypan blue stained samples were chosen and are visualized in Figure 2.

Table 1: Apoptotic and Live Cell Segmentation using trypan blue stain images

With Stain						
Types of Filter	**Recall**		**IoU**		**F-measure**	
	Apoptotic	**Live**	**Apoptotic**	**Live**	**Apoptotic**	**Live**
Basic	0.930	0.866	0.917	0.805	0.552	0.719
Gabor	0.861	0.714	0.75	0.806	0.527	0.753
Sobel	0.797	0.843	0.791	0.745	0.469	0.699
Structure Eigen	0.809	0.835	0.875	0.851	0.534	0.726

Table 2: Apoptotic and Live Cell Segmentation using images without stain

Without Stain						
Types of Filter	**Recall**		**IoU**		**F-measure**	
	Apoptotic	**Live**	**Apoptotic**	**Live**	**Apoptotic**	**Live**
Basic	0.767	0.903	0.595	0.751	0.504	0.685
Gabor	0.712	0.906	0.595	0.713	0.508	0.652
Sobel	0.672	0.908	0.595	0.559	0.472	0.551
Structure Eigen	0.681	0.896	0.595	0.636	0.476	0.539

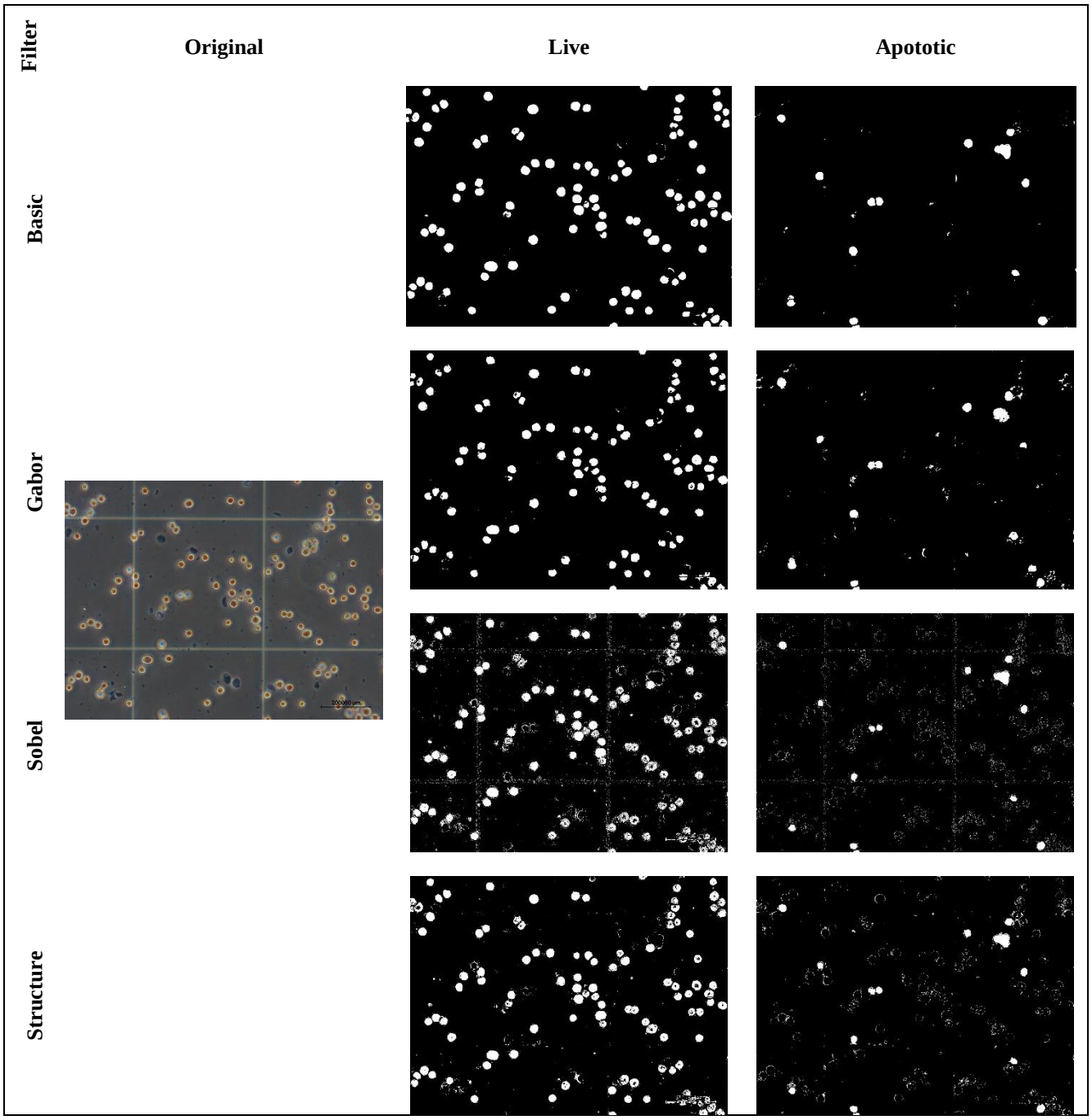

Fig 3: Segmentation of live and apoptotic cell in trypan blue stain pig luteal cell images.

Conclusion

The research illustrated the automated image segmentation using Fiji an open-source software. Through an analysis of the pixel classification algorithm applied to various cell image datasets, it was determined that cell images with trypan blue stain are more conducive to segmentation compared to unstain images. Notably, while deep learning typically demands extensive datasets, this algorithm prove advantageous for image segmentation even with limited datasets.

References

1. Ljosa V, Carpenter AE. Introduction to the quantitative analysis of two-dimensional fluorescence microscopy images for cell-based screening. PLoS Comput Biol. 2009;5(12):e1000603.
2. Eliceiri KW, Berthold MR, Goldberg IG, Ibáñez L, Manjunath BS, Martone ME, *et al*. Biological imaging software tools. Nat Methods. 2012;9(7):697-710.
3. Meijering E. Cell segmentation: 50 years down the road [life sciences]. IEEE Signal Process Mag. 2012;29(5):140-145.
4. Sommer C, Straehle C, Koethe U, Hamprecht FA. Ilastik: Interactive learning and segmentation toolkit. In: 2011 IEEE International Symposium on Biomedical Imaging: From Nano to Macro. IEEE; 2011, 230-233.
5. Ronneberger O, Fischer P, Brox T. U-net: Convolutional networks for biomedical image segmentation. In: Medical Image Computing and Computer-Assisted Intervention–MICCAI 2015. Springer International Publishing; 2015, p. 234-241.
6. Schindelin J, Arganda-Carreras I, Frise E, Kaynig V, Longair M, Pietzsch T, *et al*. Fiji: an open-source platform for biological-image analysis. Nat Methods. 2012;9(7):676-682.
7. Preibisch S, Saalfeld S, Tomancak P. Globally optimal stitching of tiled 3D microscopic image acquisitions.

Bioinformatics. 2009;25(11):1463-1465.
8. Gonzalez RC. Digital image processing. Pearson education India; c2009.
9. Healy S, McMahon J, Owens P, Dockery P, FitzGerald U. Threshold-based segmentation of fluorescent and chromogenic images of microglia, astrocytes and oligodendrocytes in FIJI. J Neurosci Methods. 2018;295:87-103.
10. Oliveira-Santos N, Silva AG, Gaêta-Araujo H, Groppo FC. Influence of binarization methods on the fractal dimension of alveolar bone using digital radiographs. Oral Surg Oral Med Oral Pathol Oral Radiol. 2023;136(5):649-655.
11. Hossain MA, Khan P, Lu CC, Clements RJ. Distributed ImageJ (Fiji): a framework for parallel image processing. IET Image Process. 2020;14(12):2937-2947.
12. Beucher S, Meyer F. The morphological approach to segmentation: the watershed transformation. In: Mathematical morphology in image processing. CRC Press; 2018. p. 433-481.
13. Song R, Zhang Z, Liu H. Edge connection-based Canny edge detection algorithm. Pattern Recognit Image Anal. 2017;27:740-747.
14. Velickova N. The benefits of learning morphological cell image analysis for medical students. In: EDUvision 2019 Modern Approaches to Teaching the Future Generations. 2019. p. 818-826.
15. Saalfeld S, Cardona A, Hartenstein V, Tomančák P. As-rigid-as-possible mosaicking and serial section registration of large ssTEM datasets. Bioinformatics. 2010;26(12):i57-i63.
16. Arganda-Carreras I, Kaynig V, Rueden C, Eliceiri KW, Schindelin J, Cardona A, *et al*. Trainable Weka Segmentation: a machine learning tool for microscopy pixel classification. Bioinformatics. 2017;33(15):2424-2426.
17. Sun G, Li S, Cao Y, Lang F. Cervical cancer diagnosis based on random forest. Int J Performability Eng. 2017;13(4):446.
18. Arzt M, Deschamps J, Schmied C, Pietzsch T, Schmidt D, Tomancak P, *et al*. LABKIT: labeling and segmentation toolkit for big image data. Front Comput Sci. 2022;4:10.
19. Breiman L. Random forests. Machine Learning. 2001;45:5-32.
20. Mbiki S, McClendon J, Alexander-Bryant A, Gilmore J. Classifying changes in LN-18 glial cell morphology: a supervised machine learning approach to analyzing cell microscopy data via FIJI and WEKA. Med Biol Eng Comput. 2020;58:1419-1430.
21. Vit P. Comparison of various edge detection techniques. Int J Signal Process Image Process Pattern Recognit. 2016;9:143-158.
22. Roslan R, Jamil N. Texture feature extraction using 2-D Gabor Filters. In: 2012 International Symposium on Computer Applications and Industrial Electronics (ISCAIE). IEEE; 2012. p. 173-178.
23. Roslan R, Jamil N. Texture feature extraction using 2-D Gabor Filters. In 2012 International Symposium on Computer Applications and Industrial Electronics (ISCAIE). 2012, December, (pp. 173-178). IEEE.
24. Lavie A, Sagae K, Jayaraman S. The significance of recall in automatic metrics for MT evaluation. In: Machine Translation: From Real Users to Research: 6th Conference of the Association for Machine Translation in the Americas, AMTA 2004, Washington, DC, USA, September 28-October 2, 2004. Proceedings 6. Springer Berlin Heidelberg; 2004. p. 134-143.
25. Ahmadzadeh A, Kempton DJ, Chen Y, Angryk RA. Multiscale iou: A metric for evaluation of salient object detection with fine structures. In: 2021 IEEE International Conference on Image Processing (ICIP). IEEE; 2021. p. 684-688.
26. Sasaki Y. The truth of the F-measure. Teach Tutor Mater. 2007;1(5):1-5.